

# NUMERICAL INVESTIGATIONS ON THE FACTORS AFFECTING TRANSPORT OF GAS PHASE PLUMES ORIGINATING FROM A RESIDUAL NAPL SOURCE IN THE SUBSURFACE

Kun Sang Lee<sup>†</sup>

Div. of Civil and Environmental Engineering  
Kyonggi University, Suwon, Kyonggi 443-760, Korea  
(received July 2004, accepted September 2004)

---

**Abstract** : Residual sources of nonaqueous-phase liquids (NAPLs) in the unsaturated zone can create soil gas plumes which act as a long-term source of soil gas and groundwater. A mathematical model is developed for predicting soil gas concentrations that are a product of gas phase plumes that originate from an immobilized NAPL in the unsaturated zone. Multiphase flow, density-dependent gas flow, and interphase mass transfer between liquid and gas are included in the model. Extensive simulations with a finite-element based numerical model were performed to estimate the soil gas phase plumes resulting from an immobilized trichloroethylene (TCE) residual located in a hypothetical laboratory-scale medium. Effects of various parameters are evaluated to highlight some of the important phenomena associated with the transport of gas phase plume in variably saturated media. The simulation results indicate that the gaseous plume is very sensitive to soil texture, the locations of the residual NAPL source and water table, and variations in infiltration and evaporation rates.

---

**Key Words** : nonaqueous-phase liquid (NAPL), unsaturated zone, residual source, transport, trichloroethylene (TCE)

## INTRODUCTION

Recently, subsurface contamination by nonaqueous-phase liquids (NAPLs) becomes a widespread problem.<sup>1)</sup> The NAPLs cause various concerns because of their persistence in the subsurface and their ability of contaminating large volumes of soil and groundwater.<sup>2)</sup> NAPLs heavier than water are referred to as dense nonaqueous-phase liquids (DNAPLs). Due to capillary forces, DNAPLs leave zones of residual contaminant suspended in the pore structure

when they flow through an unsaturated zone. Halogenated organic compounds such as trichloroethylene (TCE) are the most frequently detected contaminants in the subsurface.<sup>1)</sup> A residual NAPL in the unsaturated zone is subject to volatilization. Volatilization is the primary mass transfer mechanism by which contaminants partition from the NAPL phase to the soil gas phase. Due to its high mobility, the vapor volatilized from residual organics may lead to significant gas contamination in the surface environment for a significant amount of time.<sup>3)</sup>

Many theoretical and experimental studies have focused on the migration of NAPLs and volatilization of residual NAPLs.<sup>1,3-6)</sup> Results of

---

<sup>†</sup> Corresponding author  
E-mail: kslee@kyonggi.ac.kr  
Tel: +82-31-249-9738, Fax: +82-31-244-6300

previous studies indicate that gaseous molecular diffusion and density-driven advection may be the dominant transport mechanisms. They also concluded that boundary conditions at the ground surface can have a major impact on the subsurface distribution of contaminants. The inclusion of volatilization, water/gas partitioning is shown to be necessary for accurate determination of the fate of VOCs in variably saturated media. Modeling miscible transport of volatile organics in multiphase flow condition involves many computational difficulties. Most of previous studies, therefore, have limited applicabilities due to some of simplifications made in mathematical or numerical aspects. The importance of various factors affecting vapor migration has not been fully quantified.

The objective of this paper is to provide an insight into the relative importance of driving forces causing development and transport of soil gas phase plumes in the variably saturated subsurface resulting from the residual NAPL sources. To accomplish this objective, one used a finite-element-based numerical model using fully-coupled two-phase flow equations with advective-dispersive transport in the gaseous phase.

First, the theoretical considerations and mathematical formulations are presented. The results from a series of two-dimensional simulations are presented and discussed. Results of simulations address the impact of soil texture, the location of the residual NAPL source and water table, and variations in infiltration and evaporation rates.

## MATHEMATICAL FORMULATION

### Continuity Equation

This study considers the situation where vaporization at the residual source produces a gas mixture, and transport occurs primarily by gaseous phase advection and dispersion. One will neglect any partitioning directly between the gaseous and the solid phases as suggested by Culver *et al.*<sup>7)</sup> Mass losses due to chemical or

biological decay are also neglected.

Based on the mathematical formulations by Abriola and Pinder<sup>8)</sup>, the physical processes involved in the above situation are expressed by equations of advection-dispersion mass transport for component *i* in phase  $\alpha$ .

$$\frac{\partial(\epsilon S_{\alpha} \rho_i^{\alpha})}{\partial t} + \nabla \cdot (\epsilon S_{\alpha} \rho_i^{\alpha} \mathbf{v}^{\alpha}) - \nabla \cdot \left[ \epsilon S_{\alpha} \rho_i^{\alpha} \mathbf{D}^{\alpha} \cdot \nabla \left( \frac{\rho_i^{\alpha}}{\rho^{\alpha}} \right) \right] = \hat{\rho}_i^{\alpha} \tag{1}$$

This study considers three phases including water(*W*), NAPL(*N*), or gas(*G*) and three components or species including water(*w*), NAPL(*n*), or gas(*g*).  $\epsilon$  is the porosity,  $S$  is the fluid saturation,  $\rho_i^{\alpha}$  is the concentration of component *i* in  $\alpha$ -phase,  $\mathbf{v}$  is fluid velocity vector,  $\rho^{\alpha}$  is the  $\alpha$ -phase mass density, and  $\hat{\rho}_i^{\alpha}$  represents source or sink due to interphase mass exchange.

The dispersion coefficient  $\mathbf{D}^{\alpha}$  is the second-order tensor defined as<sup>8)</sup>

$$D_{ij}^{\alpha} = \alpha_T^{\alpha} |v^{\alpha}| \delta_{ij} + (\alpha_L^{\alpha} - \alpha_T^{\alpha}) \frac{v_i v_j}{|v^{\alpha}|} + \tau^{\alpha} D_m^{\alpha} \delta_{ij} \tag{2}$$

where  $\alpha_L$  and  $\alpha_T$  are longitudinal and transverse dispersivities,  $D_m^{\alpha}$  is molecular diffusion coefficient, and  $\delta_{ij}$  is the Kronecker delta. Empirical relationship for tortuosity( $\tau$ ) of the partially saturated porous medium developed by Millington and Quirk<sup>9)</sup> was used to determine an effective diffusion coefficient  $\tau^{\alpha} D_m^{\alpha}$ .

$$\tau^{\alpha} = \epsilon^{\frac{1}{3}} S_{\alpha}^{\frac{7}{3}} \tag{3}$$

### Mass Transfer Processes

Volatilization and water/gas partitioning, mass transfer between phases in a porous medium, represent sources of pure organic vapor. First-order relationships were used to describe the mass transfer driving force.<sup>10)</sup>

$$\hat{\rho}_n^G = C_n^G (\bar{p}_n^G - \rho_n^G) \tag{4}$$

$$\hat{\rho}_{n/w}^G = C_{n/w}^G (H\rho_n^w - \rho_n^G) \quad (5)$$

where  $\bar{\rho}_n^G$  presents the equilibrium vapor concentration of NAPL component in the gas phase and  $H$  is the dimensionless Henry's law coefficient defined as follows:

$$H = \frac{\rho_n^G}{\rho_n^w} \quad (6)$$

$C_n^G$  and  $C_{n/w}^G$  are the first-order mass transfer rate coefficients depending on many physical parameters, such as porosity, pore scale geometry, and the degree of saturation.<sup>4,6)</sup> Lumped parameter power-law relationships were used in the developed model.

$$C_n^G = \lambda^{GN} (\varepsilon S_N)^{0.5} \quad (7)$$

$$C_{n/w}^G = \lambda^{GW} (\varepsilon S_w)^{0.5} \quad (8)$$

where  $\lambda^{GN}$  and  $\lambda^{GW}$  are the rate coefficients for interphase mass transfer processes.

### Fluid Flow Equation

The average interstitial velocity vector of fluid  $\alpha$ ,  $\mathbf{v}^\alpha$  is expressed in terms of the multiphase extension of Darcy's equation.<sup>11)</sup>

$$\mathbf{v}^\alpha = -\frac{\mathbf{k}k_{r\alpha}}{\varepsilon S_\alpha \mu^\alpha} \cdot (\nabla p^\alpha - \gamma^\alpha \nabla z) \quad (9)$$

where  $p^\alpha$  is the  $\alpha$ -phase pressure,  $\gamma^\alpha$  is the specific weight of the phase ( $= \rho^\alpha g$ ),  $g$  is the gravitational acceleration,  $\mathbf{k}$  is the intrinsic permeability tensor, and  $k_{r\alpha}$  is the relative permeability.

van Genuchten<sup>12)</sup> gives the following equation to determine saturation from pressure.

$$p_c(S_c) = \frac{\rho^w g \left( S_c^{-1} - 1 \right)^n}{a} \quad (10)$$

where  $a$  and  $\eta$  are empirical parameters,  $S_e$  is the effective saturation, and  $m$  is given by

$$m = 1 - \frac{1}{\eta}.$$

The relative permeabilities of water and gas are obtained by Mualem's statistical model<sup>13)</sup> and van Genuchten's equation. The relationships can be expressed as:

$$k_{rW} = S_{eW}^\zeta \left[ \left( 1 - S_{Wt}^m \right)^m - \left( 1 - S_W^m \right)^m \right] \quad (11)$$

$$k_{rG} = S_{eG}^\varphi \left\{ \left[ 1 - \left( 1 - S_{Gt} \right)^m \right]^m - \left[ 1 - \left( 1 - S_{Gt} \right)^m \right]^m \right\} \quad (12)$$

where  $\zeta$  and  $\varphi$  are pore connectivity parameters for water and gas,  $S_{eW}$  and  $S_{eG}$  are effective saturations, and subscript  $t$  represents entrapped quantity.

## SIMULATION MODEL

The coupling of equations developed earlier give rise to a set of highly nonlinear and interdependent set of partial differential equations. The set of governing equations are numerically solved for a two-dimensional vertical cross section using the finite-element method.

In many situations, a NAPL source is often located below the ground surface. This gives rise to a long-term gaseous phase source. To investigate the effects of various factors on the gas phase concentration in a hypothetical laboratory-scale system, a number of two-dimensional simulations were conducted. Of interest in these simulations is the role that soil texture, depth to the water table, location and size of source, and infiltration and evaporation rates have on the transport of trichloroethylene in the unsaturated zone. Due to its widespread occurrence as a subsurface pollutant, TCE is used as the VOC for all the numerical simulations. Its relatively high vapor pressure, vapor density, and water

Table 1. Physical and chemical properties of fluids used in the simulations.

| Property   |                                 | Value                        |  |
|--|---------------------------------|------------------------------|--|
| Fluid properties                                   | surface tension                 | water-gas ( $\sigma_{GW}$ )  | 72.75 dyne/cm                            |
|  |                                 | NAPL-water ( $\sigma_{NW}$ ) | 31.74 dyne/cm                            |
|  |                                 | gas-NAPL ( $\sigma_{GN}$ )   | 47.5 dyne/cm                             |
|  | density                         | water ( $\rho_w$ )           | 0.9982 g/cm <sup>3</sup>                 |
|  |                                 | gas ( $\rho_g$ )             | 0.00129 g/cm <sup>3</sup>                |
|  | viscosity                       | water ( $\mu_w$ )            | 0.01 poise                               |
| gas ( $\mu_g$ )                                    |                                 | 0.0002 poise                 |  |
| Transport properties                               | molecular diffusion coefficient | water ( $D_m^W$ )            | 0.00001 cm <sup>2</sup> /sec             |
|  |                                 | gas ( $D_m^G$ )              | 0.009 cm <sup>2</sup> /sec               |
|  | mass transfer rate coefficient  | gas-NAPL ( $\lambda^{GN}$ )  | $1.154 \times 10^{-6}$ sec <sup>-1</sup> |
|  |                                 | gas-water ( $\lambda^{GW}$ ) | $1.154 \times 10^{-6}$ sec <sup>-1</sup> |
|  | equilibrium concentration       | Henry's law constant ( $H$ ) | 0.236                                    |
| saturated vapor concentration ( $\bar{\rho}_n^G$ ) |                                 | 0.0011 g/cm <sup>3</sup>     |  |

solubility, compared to other VOCs, make TCE especially suitable for this investigation. The relevant physical and chemical properties of TCE<sup>14)</sup>, water, and air, listed in Table 1, were used in all the simulations.

A typical two-dimensional laboratory-scale unconfined aquifer, that is 200 cm long and 110 cm deep, similar to that considered by Lenhard *et al.*<sup>5)</sup>, is used in these simulations as shown in Figure 1. The depth to water table elevation ranges from 60 cm to 100 cm depending on examples. A residual TCE was placed 82.5 cm from the left boundary and 7.5 cm to 37.5 cm below ground surface. This residual occupies 5 cm  $\times$  5 cm to 15 cm  $\times$  15 cm of the unsaturated zone. The physical and hydraulic prop-

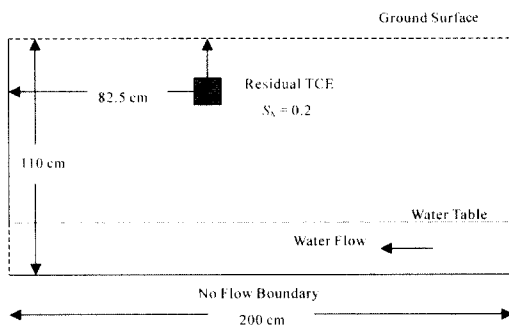


Figure 1. Domain used for TCE transport simulations.

erties of the porous media, reported by Vogel *et al.*<sup>15)</sup>, are presented in Table 2.

Boundary conditions were assigned for both water and gas flow. The lower boundary and the left and right boundary in the unsaturated zone were assumed to be impermeable to fluid flow. A boundary condition representing atmospheric gas pressure was assigned at the top. A specified fluid flux was assigned to the ground surface for the cases of infiltration or evaporation. The left and right boundaries within the saturated zone were specified water head difference of  $\Delta h_w = 0.5$  cm. All boundaries were impermeable to gas flow except for the ground surface where an atmospheric pressure was prescribed.

All inflow boundaries for water, which include the ground surface and the left saturated zone boundary, were assumed to be zero mass flux boundaries. All other boundaries were assigned zero dispersive flux conditions for aqueous phase transport. All boundaries for gas transport were treated as zero dispersive flux boundaries, except for the ground surface which was assigned stagnant boundary layer conditions.

## RESULTS OF SIMULATIONS

Fluid flow simulation was conducted with a

Table 2. Physical and hydraulic properties of the porous media used in the simulations.

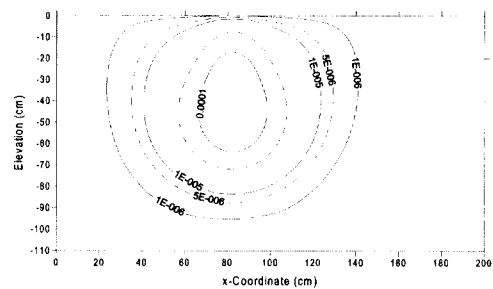
| Property             |                              |                    | Soil texture                      |                                    |                                    |
|----------------------|------------------------------|--------------------|-----------------------------------|------------------------------------|------------------------------------|
|                      |                              |                    | coarse sand                       | loam                               | silt                               |
| Field properties     | porosity ( $\epsilon$ )      |                    | 0.47                              | 0.43                               | 0.46                               |
|                      | permeability ( $k$ )         |                    | $2.1 \times 10^{-6} \text{ cm}^2$ | $2.95 \times 10^{-7} \text{ cm}^2$ | $7.09 \times 10^{-8} \text{ cm}^2$ |
| S-p model properties | scaling parameter ( $a$ )    |                    | $0.156 \text{ cm}^{-1}$           | $0.036 \text{ cm}^{-1}$            | $0.016 \text{ cm}^{-1}$            |
|                      | fitting parameter ( $\eta$ ) |                    | 4.26                              | 1.56                               | 1.37                               |
|                      | residual saturation          | water ( $S_{Hr}$ ) | 0.0                               | 0.0                                | 0.0                                |
|                      |                              | NAPL ( $S_{Nr}$ )  | 0.2                               | 0.2                                | 0.2                                |
| gas ( $S_{Gr}$ )     |                              | 0.0                | 0.0                               | 0.0                                |                                    |
| k-S model properties | pore connectivity parameter  | water ( $\zeta$ )  | 0.5                               | 0.5                                | 0.5                                |
|                      |                              | gas ( $\varphi$ )  | 0.5                               | 0.5                                | 0.5                                |

saturated medium to get an initial fluid saturation distribution. The initially water-saturated soil is allowed to drain, thereby creating a quasi-steady-state moisture profile. Quasi-steady-state conditions were reached after 7200 to 14400 seconds depending on soil texture. After reaching quasi-steady-state saturation, a residual TCE source is applied at a specified location. The simulations were carried out over a period of 8 hours. Extensive simulations with a variety of parameters were performed to examine effects of these coefficients on the transport.

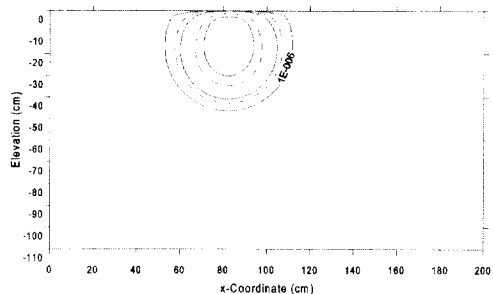
### Soil Texture

Simulations were performed to examine the importance of the soil texture characterized by physical and hydraulic properties listed in Table 2. Fig. 2 shows the concentration contour of gas phase TCE plumes for coarse sand, loam and silt at 8 hours. Solid lines represent  $1 \times 10^{-6}$ ,  $1 \times 10^{-5}$ , and  $1 \times 10^{-4} \text{ g/cm}^3$ , respectively, and dashed lines  $5 \times 10^{-6}$  and  $5 \times 10^{-5} \text{ g/cm}^3$ .

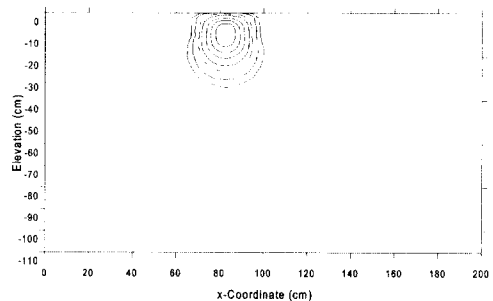
The gaseous plumes are shown to be near circular, centered very near the source. Vaporization at the source produces a gas mixture and transport will be primarily gaseous phase advection and dispersion. For the case of highly permeable texture such as coarse sand, all soil gas contours far away from the TCE source indicate vertical diffusion from the water table located on -100 cm to the atmosphere. The  $1 \times 10^{-6} \text{ g/cm}^3$  soil gas concentration contour extends more than 55 cm from the source in the hori-



(a) coarse sand



(b) loam



(c) silt

Figure 2. TCE concentration after 8 hours for different soil textures: depth to water table = 100 cm, coordinates of source location = (82.5 cm, -7.5 cm), source size = 10 cm  $\times$  10 cm.

zontal direction. Less spreading was observed in less permeable soils such as loam and silt. Slow movement of gaseous plume is due to high water saturation in the unsaturated zone and low intrinsic permeability. Hydraulic properties of a soil can therefore be taken to be a significant factor in this simulation.

**Source Size**

In order to evaluate the contribution of source size to transport, simulations were repeated for different source sizes. In the simulations performed, an immobilized TCE source was located -7.5 cm below the ground surface in areas of 5 cm × 5 cm, 10 cm × 10 cm, and 15 cm × 15 cm. Based on the simulation results, area of gas phase concentration higher than  $1 \times 10^{-6}$  g/cm<sup>3</sup> was evaluated. The source size affects the solution as expected; much larger size of TCE-contaminated area in gas phases was greater in case of a large source, as illustrated in Figure 3.

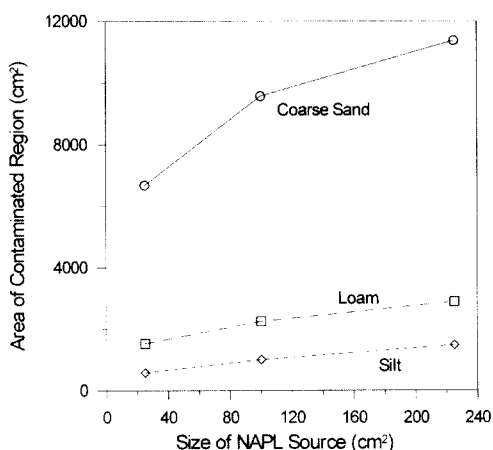


Figure 3. Area of TCE-contaminated region after 8 hours for different soil textures: depth to water table = 80 cm, coordinates of source location = (82.5 cm, -7.5 cm).

**Location of Water Table**

The importance of location of water table in TCE transport was demonstrated by comparing simulation results from three different cases. The depths to water table are 60, 80, and 100 cm

from ground surface.

The area of gas phase TCE plumes at 8 hours is shown in Figure 4. Examination of the gaseous plumes indicates that the TCE contaminated area increases when the water table is located deeper. Deeper water table results in higher gas saturation at the TCE residual. Since the dominant pathway for gaseous plume is through diffusion into the gas phase, the transport of TCE increases due to the higher gas phase saturation. In other words, volatilization becomes increasingly important as the water saturation decreases. The contaminated area, as demonstrated earlier, increases with the increasing water saturation as the source becomes larger.

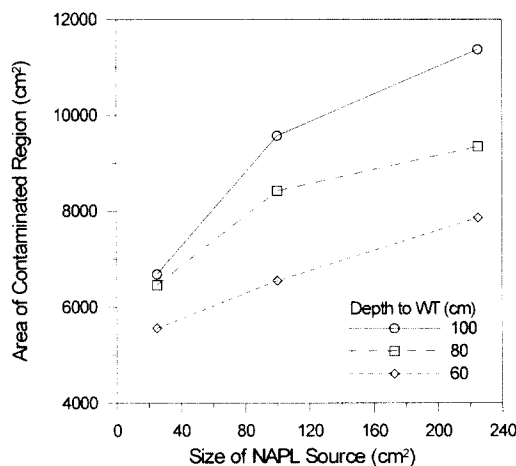


Figure 4. Area of TCE-contaminated region after 8 hours for different location of water table for coarse sand: coordinates of source location = (82.5 cm, -7.5 cm).

**Residual Source Location**

Additional simulations were performed to examine the importance of the vertical position of the source. The coordinates of exact residual locations are (82.5 cm, -7.5 cm), (82.5 cm, -22.5 cm), and (82.5 cm, -37.5 cm).

Figure 5 shows area of gas phase TCE plumes at 8 hours resulting from the TCE residual placed at various locations. Area of TCE contaminated region decreases when the contamination source is located closer to the

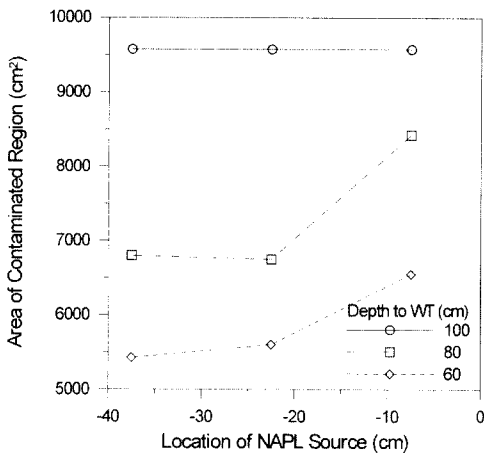


Figure 5. Area of TCE-contaminated region after 8 hours for location of NAPL source for coarse sand: depth to water table = 80 cm, source size = 10 cm × 10 cm.

water table. As the source moves closer to the water table, the area contaminated by gas plume decreases with the increasing water saturation. Being a retarding mechanism for gas phase transport, higher water saturation reduces the volatilization rate. On the other hand, diffusion directly from the source to the atmosphere is decreased when the source is moved away from the ground surface. The residual TCE placed below -22.5 cm in the unsaturated zone does not affect the rate of volatilization considerably due to these combined effects.

### Variations in Infiltration and Evaporation Rates

Infiltration or ground water recharge rates are both spatially and temporally variable, and depend on climactic, soil, and vegetative conditions.<sup>16)</sup> With all other conditions identical to the base case, Fig. 6 shows the effect of infiltration rate of  $5 \times 10^{-7} \text{ cm}^3/\text{cm}^2/\text{sec}$  to  $5 \times 10^{-5} \text{ cm}^3/\text{cm}^2/\text{sec}$  on the TCE transport in the various soil textures. The contaminated area increased slightly for all soil textures considered, as compared to those areas determined for the base case. These small changes in mass transfer rates are considered as a result of the combined effects of increased advection and higher water saturation near source.

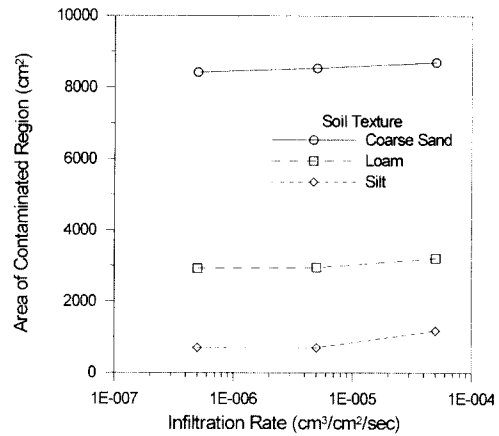


Figure 6. Area of TCE-contaminated region after 8 hours for different infiltration rate for coarse sand: depth to water table = 80 cm, source size = 10 cm × 10 cm, coordinates of source location = (82.5 cm, -7.5 cm).

To incorporate an evaporation process on the ground surface, the distribution of the phases was determined from fractional flow. Given that total evaporation rate  $q_t$  is specified, the flux of  $\alpha$  phase fluid  $q_\alpha$  is determined as

$$q_\alpha = f_\alpha q_t \tag{13}$$

where  $f_\alpha$  is the fractional flow function defined

$$\text{by mobility of each fluid } \lambda_\alpha = \frac{kk_{r\alpha}}{\mu_\alpha} .$$

$$f_\alpha = \frac{\lambda_\alpha}{\lambda_w + \lambda_G} \tag{14}$$

The simulations were carried out using total evaporation rates of  $5 \times 10^{-5} \text{ cm}^3/\text{cm}^2/\text{sec}$  to  $5 \times 10^{-3} \text{ cm}^3/\text{cm}^2/\text{sec}$  on the TCE transport through coarse sand for the various source sizes. The area of contaminated region was decreased with the inclusion of evaporation since TCE contaminated gas leaves the unsaturated zone by escaping to the atmosphere. The rate of evaporation plays very important role in the transport of TCE through the unsaturated zone into atmosphere. As shown in Figure 7, higher

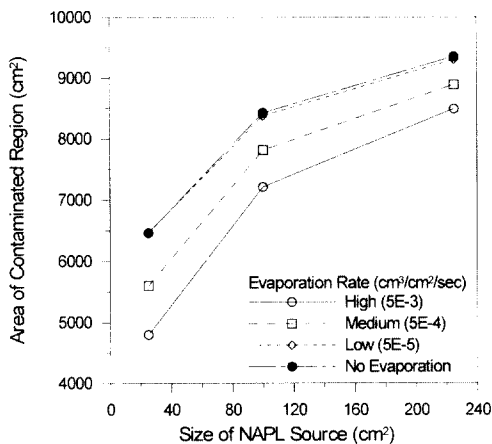


Figure 7. Area of TCE-contaminated region after 8 hours for different total evaporation rate for coarse sand: depth to water table = 80 cm, coordinates of source location = (82.5 cm, -7.5 cm).

rate of total evaporation greatly reduced the spread of the plume in gas phase.

## CONCLUSIONS

A model was developed for predicting the fate of an immobilized NAPL in the unsaturated zone. Multiphase flow, density-dependent gas flow, and interphase mass transfer between liquid and gas are included. A numerical investigation was conducted on a hypothetical laboratory-scale media involving transport of TCE. Effects of various parameters are evaluated to highlight some of the important phenomena associated with the transport of gas phase plume in variably saturated media.

High degree of soil gas concentration as a result of the TCE residual was observed for a highly permeable soil due to low water saturation in the unsaturated zone and high intrinsic permeability. Larger size of source located near ground surface with deep water table results in larger area of contamination since volatilization becomes increasingly important as the water saturation decreases. The contaminated area was decreased with the inclusion of evaporation since TCE contaminated gas escapes to the atmosphere. However, the effects of infiltration were

not significant.

## REFERENCES

- Jellali, S., Benremita, H., Muntzer, P., Razakarisoa, O. and Schafer, G., "A large-scale experiment on mass transfer of trichloroethylene from the unsaturated zone of a sandy aquifer to its interface," *J. of Contam. Hydrol.*, **19**, 31-53 (2003).
- Khachikian, C. and Harmon, T. C., "Non-aqueous phase liquid dissolution in porous media: current state of knowledge and research needs," *Transport in Porous Media*, **38**, 3-28 (2000).
- Mendoza, C. A. and Frind, E. O., 1990, "Advective-dispersive transport of dense organic vapors in the unsaturated zone: 1. model development," *Water Resour. Res.*, **26**(3), 379-387 (1990).
- Sleep, B. E. and Sykes, J. K., "Modeling the transport of volatile organics in variably saturated media," *Water Resour. Res.*, **25**(1), 81-92 (1989).
- Lenhard, R. J., Oostrom, M., Simmons, C. S. and White, M. D., "Investigation of density-dependent gas advection of trichloroethylene: experiment and a model validation exercise," *J. of Contam. Hydrol.*, **60**, 47-67 (1995).
- Thomson, N. R., Sykes, J. F. and van Vliet, D., "A Numerical investigation into factors affecting gas and aqueous phase plumes in the subsurface," *J. of Contam. Hydrol.*, **28**, 39-70 (1997).
- Culver, T. B., Shoemaker, C. A. and Lion, L. W., "Impact of vapor sorption on the subsurface transport of volatile organic compounds: a numerical model and analysis," *Water Resour. Res.*, **28**, 2259-2270 (1991).
- Abriola, L. M. and Pinder, G. F., "A multi-phase approach to the modeling of porous media contamination by organic compounds, 2. numerical simulation," *Water Resour. Res.*, **21**(1), 19-28 (1985).



9. Millington R. J. and Quirk, J. P., "Permeability of porous solids," *Trans. Faraday Soc.*, **57**, 1200-1207 (1961).
10. Nirmalakhandan, N, Modeling Tools for Environmental Engineers and Scientists, CRC Press, Boca Raton (2002).
11. Charbeneau, R. J., Groundwater Hydraulics and Pollutant Transport, Prentice Hall, Englewood Cliffs, (2000).
12. van Genuchten, M. Th., "A Closed-form equation for predicting the hydraulic conductivity of unsaturated soils," *Soil Sci. Soc. Am. J.*, **44**, 892-898 (1980).
13. Mualem, Y., "A new model for predicting the hydraulic conductivity of unsaturated porous media," *Water Resources Res.*, **12**(3), pp. 513-522 (1976).
14. Falta, R. W., Javandel, J., Pruess, K. and Witherspoon, P. A., "Density-driven flow of gas in the unsaturated zone due to the evaporation of volatile organic compounds," *Water Resour. Res.*, **25**, 2159-2169 (1989).
15. Vogel, T., van Genuchten, M. Th. and Cislerova, M., "Effects of the shape of the soil hydraulic functions near saturation on variably-saturated flow predictions," *Adv. in Water Resour.*, **24**, 133-144 (2001).
16. Yang, M. and Yanful, E. K., "Water balance during evaporation and drainage in covers under different water table conditions," *Adv. in Environ. Res.*, **6**, 505-521 (2002).